CHEMISTRY
A European Journal

www.chemeurj.org

Reprint

A Journal of
ChemPubSoc Europe
ACES
Asian Chemical Editorial Society
WILEY-VCH

ChemPubSoc Europe

DOI: 10.1002/chem.201800817

CHEMISTRY A European Journal Full Paper

Spectroscopy and Diffraction |*Hot Paper*|

Disulfuryl Dichloride $ClSO_2OSO_2Cl$: A Conformation and Polymorphism Chameleon

Angélica Moreno Betancourt,[a] Jan Schwabedissen,[b] Rosana M. Romano,*[a] Carlos O. Della Védova,[a] Helmut Beckers,[c] Helge Willner,[d] Hans-Georg Stammler,[b] and Norbert W. Mitzel*[b]

Abstract: Disulfuryl dichloride $ClSO_2OSO_2Cl$ was characterized by vibrational spectroscopy in the gaseous and liquid phase as well as in the Ar-matrix. By varying the temperature, certain bands could be assigned to several conformers. Gas-phase electron diffraction revealed a dominance of the *anti*-conformer at ambient temperature. The same conformation was found in the solid state. Via the in situ technique for crystallization, not less than four different modifications were identified. Among these different modifications, the structural parameters of the molecules remain relatively constant, but the aggregation pattern changes. Although the molecules aggregate by chlorine···oxygen contacts in each modification, the geometrical parameters of these interaction show significant differences and were evaluated and are in part inconsistent with the halogen bonding concept.

Introduction

Disulfuryl dichloride, $ClSO_2OSO_2Cl$, can be synthesized in a photochemical reaction of Cl_2 and O_2 with SO_2.[1] Thus, this reaction can take place in the Venusian atmosphere, where high concentrations of chlorine gas are found.[2] A photochemical reaction yielding the peroxo-bridged disulfuryl dichloride, $ClSO_2OOSO_2Cl$, confirms this[3] and provides an explanation of the relatively low concentration of oxygen in Venus' atmosphere. A previous study on the photochemical properties of disulfuryl dichloride[4] revealed its high thermal and photochemical stability. Although the title compound is known for more than a century[5] no complete elucidation of its spectroscopic or structural features was undertaken. Contrary to that, the corresponding disulfuryl difluoride, FSO_2OSO_2F, has been characterized spectroscopically[1,6] and structurally—first in the gas phase[7] and later also in the solid state.[8] In the gas phase the difluoride solely consists of an *anti*-conformer with a torsional angle ϕ(FS···SF) of 119.1(6)°, whereas in the solid state this torsional angle measures 144.9(1)° while no pronounced individual interactions amongst the molecules can be identified.

Herein, we report for disulfuryl dichloride, $ClSO_2OSO_2Cl$, the spectroscopic properties in the liquid, the gas phase and in Ar-matrix isolation as well as the structures determined in the solid state by X-ray diffraction on in situ grown crystals and in the gas phase by electron diffraction of free molecules.

Results and Discussion

For the determination of possible conformers in the gas phase a potential-energy scan was performed on the O3LYP[9] level of density-functional theory with the correlation consistent cc-pVTZ[10] basis set (Figure 1). On this fourfold symmetric energy-surface, three distinguishable conformers were located. The lowest-energy *anti*-conformer is of C_2 symmetry and has both dihedral angles ϕ(Cl1-S1-O1-S2) and ϕ(Cl2-S2-O1-S1) of about 80° and a dihedral angle along the S···S vector, ϕ(Cl–S···S–Cl), of 152°. The *syn*-conformer is the next lowest in energy; its dihedral angles ϕ(Cl1-S1-O1-S2) and ϕ(Cl2-S2-O1-S1) measure 70° and 250° (equivalent to 110°). This conformer adopts a torsional angle ϕ(Cl–S···S–Cl) of 37°. The highest-energy minimum corresponds to the *gauche*-conformation with dihedral angles

[a] *Dr. A. Moreno Betancourt, Prof. Dr. R. M. Romano, Prof. Dr. C. O. Della Védova, CEQUINOR (UNLP-CONICET, CCT La Plata), Departamento de Química, Facultad de Ciencias Exactas, Universidad Nacional de La Plata, La Plata CP 1900 (Argentina), E-mail: romano@quimica.unlp.edu.ar*

[b] *Dr. J. Schwabedissen, Dr. H.-G. Stammler, Prof. Dr. N. W. Mitzel, Fakultät für Chemie, Lehrstuhl für Anorganische Chemie und Strukturchemie, Centrum für molekulare Materialien CM2, Universität Bielefeld, Universitätsstr. 25, 33615 Bielefeld (Germany), E-mail: mitzel@uni-bielefeld.de*

[c] *Dr. H. Beckers, Institut für Chemie und Biochemie, Anorganische Chemie, Freie Universität Berlin, Fabeckstraße 34-36, 14195 Berlin (Germany)*

[d] *Prof. Dr. H. Willner, FB C-Anorganische Chemie, Bergische Universität Wuppertal, Gaußstraße 20, 42097 Wuppertal (Germany)*

Supporting information and the ORCID identification number(s) for the author(s) of this article can be found under: https://doi.org/10.1002/chem.201800817.

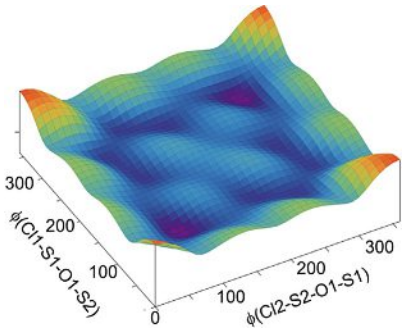

Figure 1. Potential energy surface for the rotations about the S1–O1 and S2–O1 axes by independently varying the two dihedral angles ϕ(Cl1-S1-O1-S2) and ϕ(Cl2-S2-O1-S1). Atom numbering is presented in Figure 2.

Table 1. Structural parameters of the different conformers calculated at the MP2[11]/cc-pVTZ level of theory.

Parameter	*anti*	*syn*	*gauche*
r(O1–S1)	1.654	1.654	1.648
r(O1–S2)	1.654	1.652	1.665
r(S1–Cl1)	2.027	2.019	2.015
r(S2–Cl2)	2.027	2.020	2.012
∡(S1-O1-S2)	122.2	124.2	119.4
∡(O1-S1-Cl1)	98.8	100.4	99.6
∡(O1-S2-Cl2)	98.8	97.7	93.9
ϕ(Cl1-S1-O1-S2)	78.8	66.2	86.5
ϕ(Cl2-S2-O1-S1)	78.8	108.2	163.9
ϕ(Cl2-S2···S1-Cl1)	151.9	38.4	78.7
Abundance, %	70.4	16.3	13.3

Distances *r* in Å, angles ∡ and dihedrals ϕ in degrees.

ϕ(Cl1-S1-O1-S2) and ϕ(Cl2-S2-O1-S1) of 90° and 190°(equivalent to 170°), and ϕ(Cl–S···S–Cl) of 83°. All conformers are depicted in Figure 2 and the calculated structural parameters are listed in Table 1.

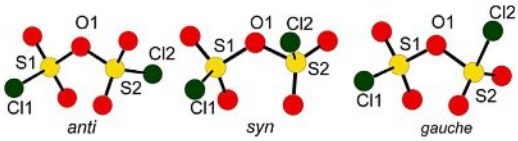

Figure 2. Calculated structures of the different conformers of $ClSO_2OSO_2Cl$.

Corresponding structure parameters of the three conformers depend on their torsional angles as well as on their central S-O1-S angle. For example, in the *gauche*-conformer the S1–O1 bond (1.665 Å) is longer at than the corresponding bond S2–O1 (1.648 Å) to the sulfuryl group, while the S–Cl bond is nearly in-plane with the S-O1-S unit. The smallest S1-O1-S2 angle (119.4°) is also observed in the *gauche*-conformer.

Vibrational spectroscopy

Intensive studies on the vibrational properties of molecules containing the S-O-S moiety have been carried out in the 1960s.[1,6,12] In here, infrared spectroscopy of the gas and Raman spectroscopy of the liquid phase of disulfuryl dichloride along with matrix isolation infrared spectroscopy were used to determine the conformational behavior in the different phases. Therefore, experimental spectra are compared to theoretical ones at the B3P86/6-31G(d)[13,14] level of theory. Figure 3 shows the FTIR and FT Raman spectra at 20 °C in comparison with the computed ones for the different conformers; Table S4 contains a detailed listing of the vibrational frequencies with a new assignment as well as the one of previous investigations.

As the recorded spectra show less bands than for the preceding investigations,[15] the bands were assigned de novo.[5] The smaller number of bands indicates a higher purity of the sample used here. Despite the additional bands present in the reported vibrational spectra, there is a good agreement between the present spectra and the reported ones.[15] The authors report a single band for $\tilde{\nu}_{as}(SO_2)$ at 1470 cm^{-1} and both

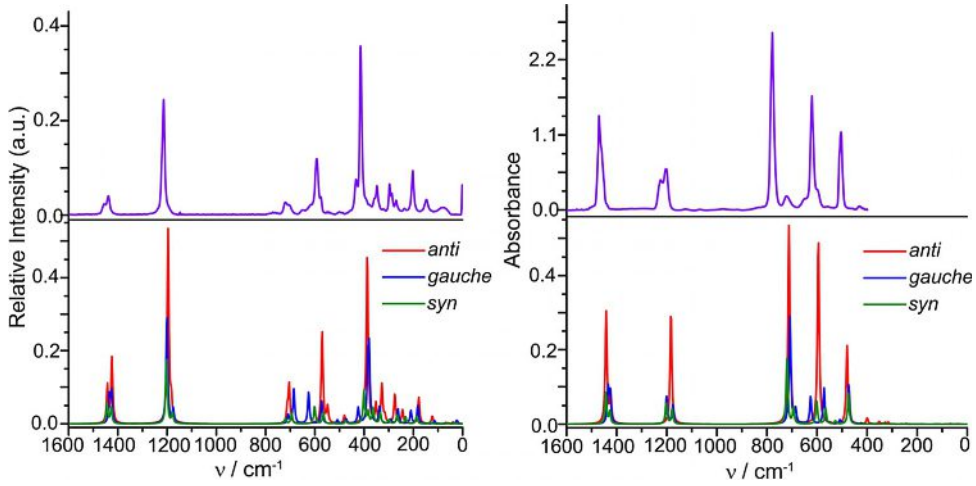

Figure 3. Raman spectrum of the liquid (left) and infrared spectrum of the gas (right) of $ClSO_2OSO_2Cl$. The upper traces (blue) show experimental and the lower show the spectra of the different conformers are weighted according to the equilibrium abundance at 20 °C according to the B3P86/6-31G(d) level of theory.

symmetric stretching modes of the SO_2 unit to appear at 1225 and 1201 cm^{-1}. In the Raman spectrum some bands differ slightly from the bands assigned by Gillespie.[1] For example, the antisymmetric stretching modes of the SO_2 group are now found at 1455 and 1438 cm^{-1}; they were earlier assigned to 1462 and 1442 cm^{-1}. In the symmetric stretching mode region only one band at 1214 cm^{-1} is observed in the present Raman spectrum while in the previous work two bands, at 1209 and 1189 cm^{-1}, were assigned to these modes. However, for a more thorough investigation of the conformational composition we recorded matrix infrared spectra of isolated species at cryogenic temperatures (15 K) for different inlet temperatures. Some representative spectra are shown in Figure 4.

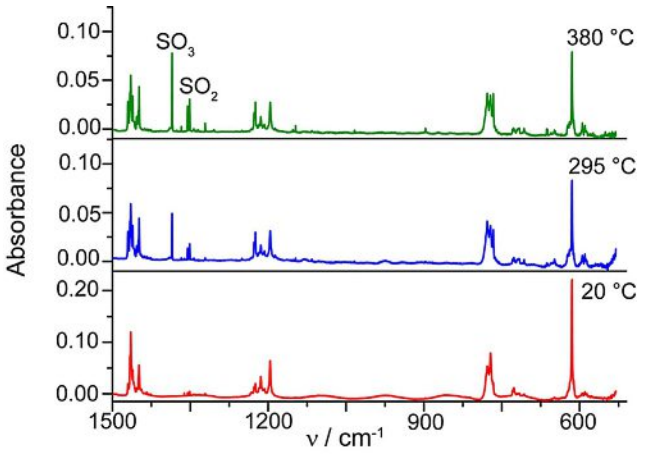

Figure 4. FTIR spectra of $ClSO_2OSO_2Cl$ isolated in an argon matrix. The samples were heated to the shown temperatures directly prior to deposition on the cold window.

The effect of heating is not only the increase of the relative intensity of the bands of the less abundant conformers but also decomposition of the compound under investigation. This is observed in form of the peaks at about 1350 cm^{-1}, which are the characteristic bands of sulfur dioxide and trioxide.[17] Figure 5 shows enlargements of two different regions of the matrix IR spectra.

The region between 1475 and 1440 cm^{-1} shows the asymmetric stretching vibrations of the SO_2 unit ($\tilde{\nu}_{as}(SO_2)$). Bands are assigned according to the relative changes upon heating. The symmetric stretching modes are observed in the interval between 1240 and 1180 cm^{-1}. As expected the relative intensities of the bands belonging to the lowest-energy conformer, *anti*, decrease when the mixture is heated. In the left part of Figure 5 this behavior is seen for the band at 1465 cm^{-1}; thus, this belongs to the *anti*-conformer. The band at 1449 cm^{-1} corresponds to the *gauche*-conformer as it is becoming more intense upon heating relative to bands of the *anti*-conformer. The bands at 1227 and 1224 cm^{-1} are assigned to the *syn*- and *gauche*-conformers, respectively, as the computed values of the absorption coefficients are much larger for these conformers than for the *anti*-conformer, to which the band at 1222 cm^{-1} was assigned. At 1192 cm^{-1} an overtone of the deformation vibration of the SO_2 group of the *anti*-conformer is observed, which is intensified due to Fermi resonance with the $\tilde{\nu}_s(SO_2)$ fundamental mode. Other bands in the spectra were analyzed in a similar way based on the computed frequencies and the intensities changing at different temperatures. Table S4 summarizes the assignments of the vibrational bands to the different conformers.

Gas-phase structure

The structure of free molecules of disulfuryl dichloride was determined by means of gas electron diffraction (GED; Figure 6). Details of the procedure are described in the Experimental Section. In the refinement, the three different conformers were initially included and their contributions weighted according to the differences in energy at the MP2/cc-pVTZ level of theory. For the conformer being lowest in energy (*anti*) C_2 symmetry was assumed while the other two possible conformers were described in C_1 symmetry. During the refinement, the amounts of conformers were varied without any restrictions. Initially, the bonded distances were refined successively in three individual groups. As a next parameter the $\angle$(S-O1-S) angle was included in the refinement followed by two groups of $\angle$(O_t-S-O_t) angles, one with higher and the other one with lower values. Subsequently the angles $\angle$(O1-S-Cl) were refined in a group and all

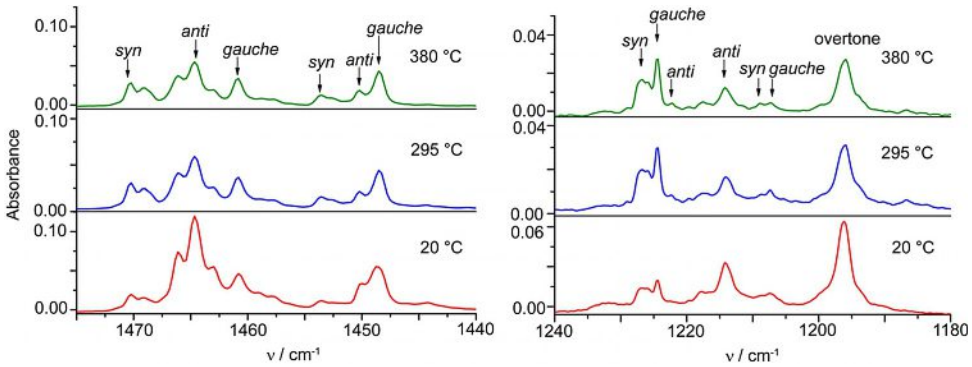

Figure 5. Different regions (right: 1180–1240 cm^{-1}; left: 1440–1475 cm^{-1}) of the IR spectra of isolated molecules of $ClSO_2OSO_2Cl$ in an argon matrix at 15 K. The mixture of the inert gas and the sample was heated prior to ablation to the shown temperatures.

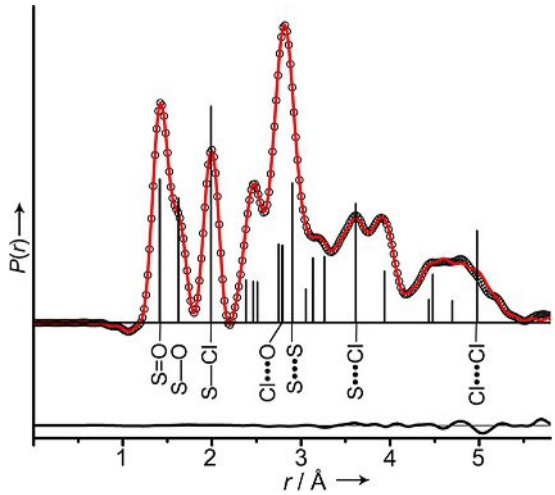

Figure 6. Radial distribution curve based on the GED structure refinement of $ClSO_2OSO_2Cl$: experimental values (circles), model (solid line) and difference curve (lower trace, experimental minus modelled). Vertical sticks represent interatomic distances (selected are labelled).

Table 2. Structural parameters of the gas-phase structure of $ClSO_2OSO_2Cl$.

Parameters	r_e, ∡$_e$	r_g	l
r(S–Cl)	1.985(1)[1]	1.992(1)	0.0504[8]
r(S=O_1)	1.408(1)[2]	1.413(1)	0.0400[9]
r(S=O_2)	1.412(1)[2]	1.417(1)	0.0399[9]
r(S–O1)	1.617(1)[3]	1.626(1)	0.0475[10]
∡(O1-S-Cl)	98.7(3)[4]		
∡(O=S=O)	125.1(2)[5]		
∡(S-O-S)	127.2(2)[6]		
ϕ(S-O-S-Cl)	80.5(4)[7]		
ϕ(Cl–S···S–Cl)	155.2(9)[a]		

Distances r in Å, angles ∡ and dihedral angles ϕ in deg, Numbers as superscript indicate the groups the parameters were refined in. [a] Dependent parameter. r_e distance between equilibrium nuclear positions, r_g thermal averaged internuclear distance, l amplitude of vibration.

∡(Cl-S-O_t) angles were grouped together. The dihedral angles ϕ(S-O1-S-Cl) were refined separately for each conformer and in the conformers of C_1 symmetry the dihedral angles were refined individually with restraints to their computational values. Altogether, this resulted in three groups of bonded distances, five groups of angles, five groups of dihedral angles and nine groups of amplitudes, which were refined independently.

The refinement using a three-conformer model resulted in large correlations among the different types of parameters, for example, amplitudes and amounts of the conformers in the gas phase. This led some refined parameters to adopt chemically unreasonable values and the refinement resulted in a disagreement factor of more than $R_f = 5.0\,\%$. The presence of other conformers, as was proven by spectroscopy (see above) could neither be confirmed nor excluded by GED on the level of significance. Thus, we decided to use a one-conformer model to describe the experimental scattering data. Such a model for the *anti*-conformer gave a satisfactory agreement with the experimental electron diffraction data with an $R_f = 3.39\,\%$. The gas-phase structural parameters are listed in Table 2.

The conformation of gaseous disulfuryl dichloride is defined by the torsional angle ϕ(Cl–S···S–Cl). Its value of 155.2(9)° agrees well with the calculated parameter (151.9°). The difference regarding the structures in the solid state, in particular deviation from C_2 symmetry in the solid state, is due to the formation of asymmetric halogen bonds (vide infra). Regarding the conformation the characteristic parameters in the gas phase are within the range found in the solid state of the different polymorphs and in good accordance with the averaged values of structure: ϕ(Cl–S···S–Cl) (gas/solid$_{average}$/range) = 155.2(9)°/153.8°/148.0(1)° to 162.0(1)° and ϕ(S-O-S-Cl) = 80.5(4)°/80.7°/, 77.1(2)° to 86.0(1)°. Comparing the thermally averaged bonded distances S–O1 in the gas phase (1.626(1) Å) to the analogous ones in the solid state (average 1.627 Å ranging from 1.620(1) Å to 1.634(2) Å) this is in good agreement. On the other hand, the S–Cl distance in the solid state (average 1.973 Å) is by 0.02 Å shorter than the corresponding one in the gas phase. The central angle at oxygen ∡(S-O-S) deviates with 127.2(2)° from an ideal angle at a twofold substituted. This deviation can be attributed to the higher steric demand of the chlorosulfuryl group or to a conjugation effect resulting in some double bond character of the S–O1 bond. In the solid state, the angle ∡(S-O-S) is about three degrees narrower (average: 124.4°).

In Table 3 parameters of gas-phase structures of comparable molecules are listed. For of all three symmetrically substituted disulfuryl compounds a one-conformer model was used to describe the gas-phase composition. Regarding the conformational behavior the two examples in the literature, FSO_2OSO_2F[7] and $CF_3SO_2OSO_2CF_3$,[18] and the here examined $ClSO_2OSO_2Cl$ show *anti*-conformations regarding the positions of the halogen atoms or the trifluoromethyl group relatively to the S···S vector. The largest dihedral angle ϕ(S-O-S-X) is found in the trifluoromethyl compound (99.1(14)°), followed by the dichloride (80.5(4)°) and the difluoride (73.7(24)°). The same trend is ob-

Table 3. Characteristic structural parameters of symmetrically substituted disulfuryl compounds and sufuryl chloride in the gas phase.

Parameter		X	r(O1–S)	r(S–X)	∡(S-O-S)	∡(O1-S-X)	∡(O$_t$-S-O$_t$)	ϕ(S-O-S-X)	Ref.
FSO_2OSO_2F	r_g	F	1.611(5)	1.525(5)	123.6(5)	102.4(18)	128.5(14)	73.7(24)	[7]
$CF_3SO_2OSO_2CF_3$	r_a	C	1.623(5)	1.848(6)	128.1(14)	99.1(14)	128.0(21)	99.1(14)	[18]
SO_2Cl_2[a]	r_g	Cl		2.012(4)		100.3(2)	123.5(2)		[19]
$ClSO_2OSO_2Cl$	r_g	Cl	1.626(1)	1.992(1)	127.2(2)	98.7(3)	125.1(2)	80.5(4)	here

Distances r in Å, angles ∡ and dihedral angles ϕ in deg. [a] The angle ∡(O1-S-X) refers to the ∡(Cl-S-Cl).

served for the central angle ∡(S-O-S) which rises from the difluoride (123.6(5)°) to the dichloride and the trifluoromethyl species (127.2(2)° and 128.1(14)°, respectively), which are the same within the error limits. Both angles reflect the steric demand of the substituents, which rises from fluorine over chlorine to CF_3. The bond to the central oxygen atom elongates along the series FSO_2OSO_2F, $CF_3SO_2OSO_2CF_3$ and $ClSO_2OSO_2Cl$, whereas the latter two are the same within the error limits. This structural feature reflects the decreasing double bond character in the central sulfur–oxygen bond along this series. The gas-phase structure of sulfuryl chloride[19] shows a slightly longer S–Cl bond and a shorter angle regarding the terminal oxygen atoms (123.5(2)°) compared to the disulfuryl dichloride (125.1(2)°).

Structures in the solid state

Suitable crystals of disulfuryl dichloride were grown in situ in a flame sealed capillary directly on the diffractometer. The capillary was heated and cooled several times applying different temperature programs (see Experimental Section). In this way, we obtained not less than four different modifications from the identical sealed sample of the title compound and determined the crystals structure of each of these modifications plus additionally a crystal structure of oxonium perchlorate. For crystallographic details see Table 9. All four modifications exhibit approximately the same intramolecular structural parameters; a full listing is given in Table 4; Figure 7 depicts the molecular structures of modifications 1 and 2. The molecules of $ClSO_2OSO_2Cl$ aggregate via O···Cl interactions of the sigma-hole type (see below for detailed discussion), the structural parameters of these non-covalent interactions below the sum of vdW-radii of 3.32 Å are listed in Table 5 and are depicted in Figure 15. The aggregation of the four modifications is shown in Figures 8–14.

Modifications 1–3 are monoclinic, space group $P2_1/c$, the fourth is triclinic, space group $P\bar{1}$. The four different modifications can be subdivided into two pairs regarding the number

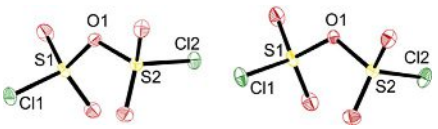

Figure 7. Molecular structure showing atom labelling in modifications 1 (left) and 2 (right) of $ClSO_2OSO_2Cl$.

Table 5. Full listing of the O···Cl interactions below 3.32 Å in the solid state of $ClSO_2OSO_2Cl$. Distances *r* in Å and angles in degree.

Number	*r*(Cl···O)	∡(SCl···O)	∡(SO···Cl)	*r*(S–Cl)
❶a	2.974(1)	165.5(1)	141.6(1)	1.972(1)
❶b	2.937(1)	177.7(1)	144.5(1)	1.971(1)
❶c	3.244(1)	99.6(1)	135.8(1)	1.972(1)
❶d	3.292(1)	105.8(1)	154.8(1)	1.972(1)
❷a	2.997(1)	164.2(1)	144.3(1)	1.966(1)
❷b	3.006(1)	171.6(1)	146.8(1)	1.973(1)
❷c	3.291(1)	101.8(1)	127.5(1)	1.973(1)
❷d	3.256(1)	104.2(1)	154.6(1)	1.966(1)
❸a	2.997(1)	173.1(1)	135.3(1)	1.971(1)
❸b	2.947(1)	167.8(1)	145.0(1)	1.972(1)
❸c	2.893(1)	164.7(1)	174.9(1)	1.967(1)
❸d	3.031(1)	172.5(1)	149.4(1)	1.975(1)
❸e	3.133(1)	101.8(1)	164.9(1)	1.972(1)
❸f	3.183(1)	100.6(1)	156.8(1)	1.975(1)
❸g	3.243(1)	103.7(1)	146.0(1)	1.967(1)
❸h	3.203(1)	156.3(1)	133.8(1)	1.976(1)
❸i	3.218(1)	137.3(1)	120.6(1)	1.976(1)
❸j	3.288(1)	97.7(1)	155.5(1)	1.979(1)
❹a	2.990(2)	173.2(1)	135.7(1)	1.973(1)
❹b	2.957(2)	168.5(1)	144.5(1)	1.972(1)
❹c	2.887(2)	164.9(1)	174.9(1)	1.969(1)
❹d	3.008(2)	171.8(1)	150.0(1)	1.975(1)
❹e	3.149(2)	102.8(1)	158.1(1)	1.972(1)
❹f	3.164(2)	99.9(1)	163.5(1)	1.975(1)
❹g	3.214(2)	137.5(1)	120.4(1)	1.977(1)
❹h	3.240(2)	155.9(1)	132.7(1)	1.977(1)
❹i	3.236(2)	103.1(1)	147.2(1)	1.969(1)
❹j	3.292(2)	100.7(1)	135.8(1)	1.969(1)
❹k	3.289(2)	98.5(1)	154.5(1)	1.977(1)

Table 4. Structural parameters of $ClSO_2OSO_2Cl$ in the different modifications.

Modification	1	2	3			4		
Molecule			1	2	3	1	2	3
r(O1–S1)	1.630(1)	1.625(1)	1.624(1)	1.620(1)	1.626(1)	1.626(2)	1.634(2)	1.628(2)
r(O1–S2)	1.628(1)	1.633(1)	1.629(1)	1.633(1)	1.624(1)	1.625(2)	1.626(2)	1.624(2)
r(S1–O2)	1.413(1)	1.411(1)	1.411(1)	1.412(1)	1.411(1)	1.413(2)	1.411(2)	1.409(2)
r(S1–O3)	1.412(1)	1.410(1)	1.409(1)	1.410(1)	1.413(1)	1.405(2)	1.405(2)	1.410(2)
r(S1–Cl1)	1.972(1)	1.973(1)	1.971(1)	1.979(1)	1.972(1)	1.973(1)	1.969(1)	1.972(1)
r(S2–O4)	1.412(1)	1.410(1)	1.411(1)	1.411(1)	1.410(1)	1.412(2)	1.413(2)	1.416(2)
r(S2–O5)	1.412(3)	1.412(1)	1.409(1)	1.411(1)	1.412(1)	1.406(2)	1.412(2)	1.408(2)
r(S2–Cl2)	1.971(1)	1.966(1)	1.976(1)	1.967(1)	1.975(1)	1.977(1)	1.977(1)	1.975(1)
∡(S1-O1-S2)	124.4(1)	124.7(1)	124.0(1)	124.5(1)	125.0(1)	124.1(1)	124.1(1)	124.9(1)
∡(O1-S1-Cl1)	100.0(1)	100.5(1)	100.7(1)	101.3(1)	101.3(1)	100.7(1)	101.4(1)	101.2(1)
∡(O1-S2-Cl2)	100.1(1)	100.2(1)	101.1(1)	101.4(1)	101.0(1)	101.0(1)	101.3(1)	101.1(1)
ϕ(S1-O1-S2-Cl2)	85.5(1)	86.0(1)	77.6(1)	77.2(1)	82.7(1)	77.9(2)	78.6(2)	82.4(2)
ϕ(S2-O1-S1-Cl1)	84.8(1)	82.0(1)	81.0(1)	78.4(1)	81.2(1)	80.6(2)	77.1(2)	81.4(2)
ϕ(Cl2-S2···S1-Cl1)	162.0(1)	159.8(1)	151.0(1)	148.0(1)	155.4(1)	150.9(1)	148.1(1)	155.4(1)

Distances *r* in Å, angles ∡ and dihedral angles ϕ in degree.

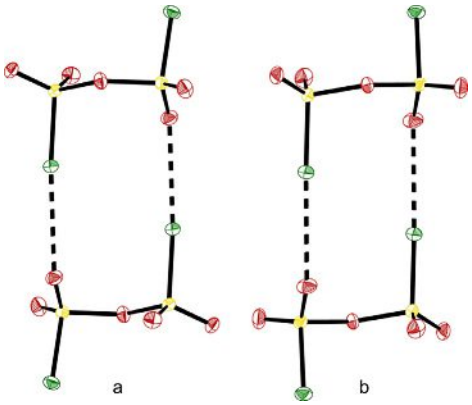

Figure 8. Dimers of (a) modification 1 and (b) modification 2 of $ClSO_2OSO_2Cl$.

of molecules contained in the asymmetric unit. Modifications 1 and 2 contain one molecule per asymmetric unit; modifications 3 and 4 contain three crystallographically independent molecules. The packing in modification 1 is more dense, it has the highest density (2.234 g cm^{-3}) of all four modifications, while the other three have lower, but very similar ones (modifications 2–4: 2.211, 2.212, 2.211 g cm^{-3}). Additionally modifications 3 and 4 show two very similar unit cell axes: 7.619 and 7.612 Å, and 9.441 and 9.447 Å. There are thus in total eight independently structurally characterized molecules of $ClSO_2OSO_2Cl$.

Modifications 1 and 2 contain primarily dimeric aggregates of inversion symmetry, by two intermolecular, symmetrically identical O···Cl interactions (❶a & ❷a) resulting in ten-membered rings, which are nearly congruent for both modifications as can be seen in Figure 8. The aggregation pattern to the next molecules differs significantly as can be seen in Figure 9.

As the result the aggregation motif of both modifications shows four dimers forming a 22-membered ring via O···Cl contacts ❶b and ❷b, by involving alternatingly one dimer with a molecular unit site and one with an aggregated site, but differing in the orientation of the dimers to each other as shown in Figure 10 and 11. The layers shown in Figure 11 are further interconnected by weaker Cl···O contacts longer than 3.2 Å.

In modifications 3 and 4 inversion symmetric tetramers are formed by two symmetrically unique Cl···O contacts (❸a & ❸c and ❹a & ❹c) forming 18-membered rings, see Figure 12. These tetramers are formed by each monomer contributing one O and one Cl atom for interactions, however, alternatingly so that one monomer uses O and Cl atoms of the same SO_2Cl group and the other monomer contributes with the either the O or Cl atom from each of its two SO_2Cl moiety in the other crystallographic unique monomer. The angles of both unique Cl···O connecting vectors of ❸a and ❸c as well as of ❹a and ❹c are 113.8(1)° in both modifications. These tetramers are connected to other tetramers by two crystallographically equivalent monomers of $ClSO_2OSO_2Cl$ contributing with both their chlorine atoms (Cl···O contacts: ❸b & ❸d and ❹b & ❹d, Figure 13) forming a 28-membered ring involving eight $ClSO_2OSO_2Cl$ molecules in the same way for both modifications building a rope-ladder-like motif, see Figure 13.

The difference between both modifications 3 and 4 is not clear without considering the arrangement of these ladders relative to each other. The weaker O···Cl interactions, that is, ❸e and ❸f or ❹e and ❹f, interconnect the rope ladders in different ways. No additional O···Cl interactions below 3.32 Å can be found. For better visibility a plane defined by the four σ-

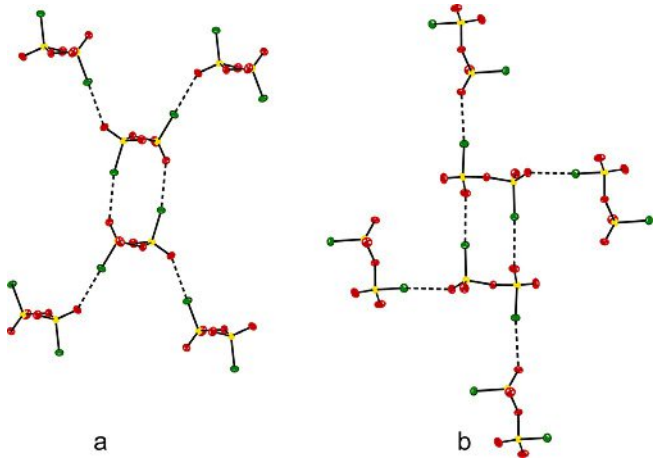

Figure 9. Aggregation of dimers of $ClSO_2OSO_2Cl$ in (a) modification 1 and (b) modification 2.

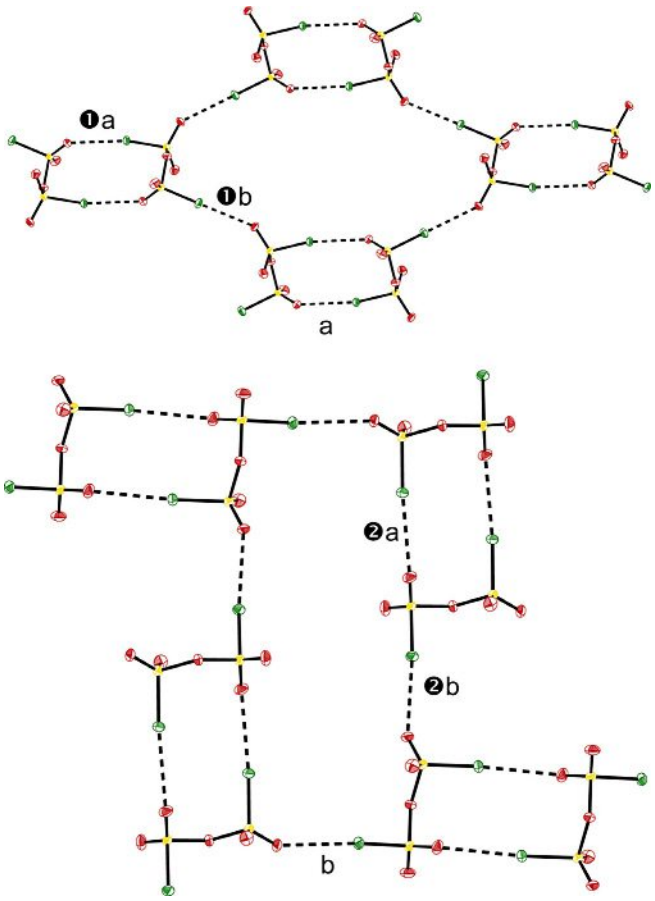

Figure 10. Tetrameric arrangement of the dimers of $ClSO_2OSO_2Cl$ in (a) modification 1 and (b) modification 2.

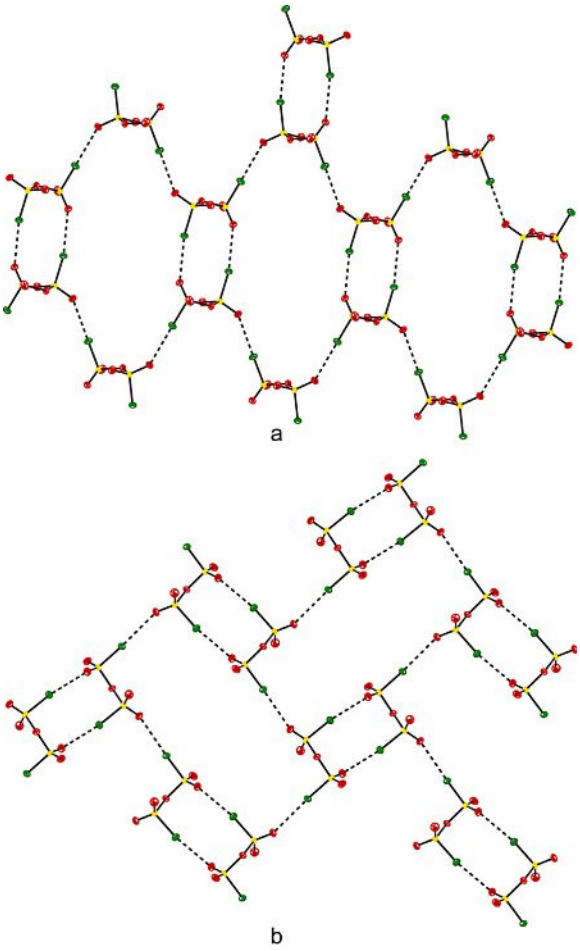

Figure 11. Layer structure of (a) modification 1 and (b) modification 2 of $ClSO_2OSO_2Cl$.

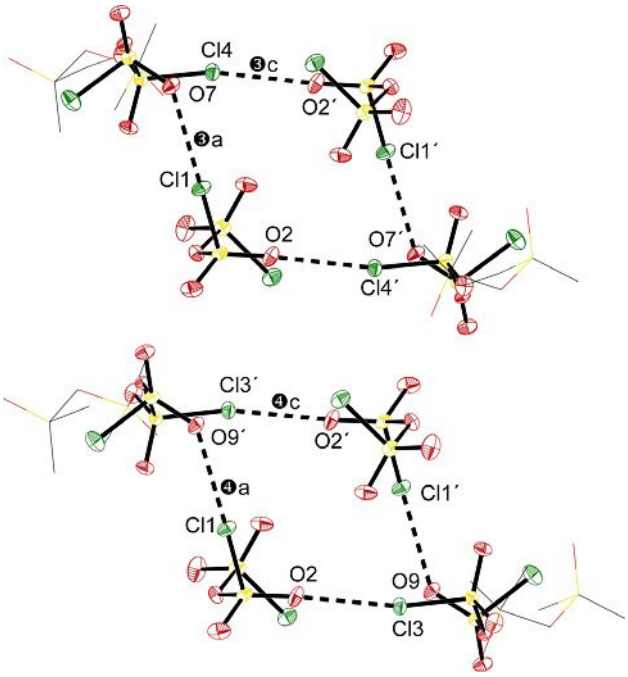

Figure 12. Inversion symmetric tetramers in the extended solid-state structure of modification 3 (left) and modification 4 (right) of $ClSO_2OSO_2Cl$.For reasons of clarity the third molecule in the asymmetric unit is wire framed.

hole-bonded chlorine atoms of the tetramers is shown in Figure 14. These planes must be all parallel in triclinic modification 4, whereas monoclinic modification 3 shows an angle of 15.0(1)° between the planes of two different rope ladders.

Concerning the molecular structures, the central S–O bonds vary between 1.620(1) and 1.634(2) Å. The range for the S–Cl bonds is 1.966(1) to 1.979(1) Å. The central S1-O1-S2 angle varies from 123.9(1)° to 125.0(1)°. The dihedral angles ϕ(Cl1-S1-O1-S2) and ϕ(Cl2-S2-O1-S1) adopt values between 86.0(1)° and 77.2(1)°. The mean value is in good agreement with the calculated minimum structure adopting a dihedral angle of 78.8° at the MP2/cc-pVTZ level of theory. In comparison to the gas-phase structure of $ClSO_2OSO_2Cl$ the dihedral angle (80.5(4)°) lies within the range of the solid-state parameter. Note that the related disulfuryl difluoride, FSO_2OSO_2F,[8] adopts C_2 symmetry in the solid state. Its central S–O bonds at 1.610(1) Å are shorter by about 0.01 Å than the shortest measured here in the chlorine analogue. This might be due to higher group electronegativity of the fluorosulfuryl group.

However, the variation of crystallographic parameters for $ClSO_2OSO_2Cl$ by more than 0.01 Å for the different molecules show, that such a difference should not be over-interpreted, as for FSO_2OSO_2F only one modification is known, and we do not know if the structural values would also vary in a similar range for other possible modifications. Similarly, the central S-O-S angle in the difluoride at 123.4(1)° is 1° smaller than the average angle of the value among the four modifications (123.9(1)°). The only clear difference is the Cl–S···S–Cl dihedral angle along the S···S connecting vector; this is by 15° smaller

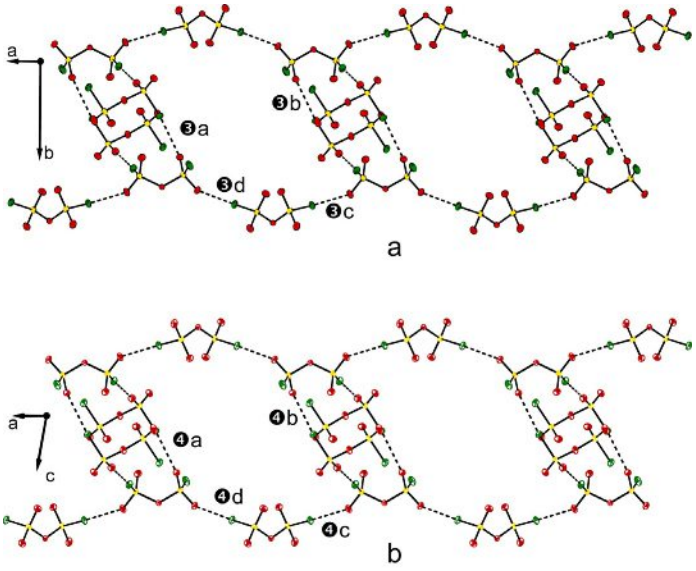

Figure 13. Rope ladder motif of (a) modification 3 and (b) modification 4 of $ClSO_2OSO_2Cl$.

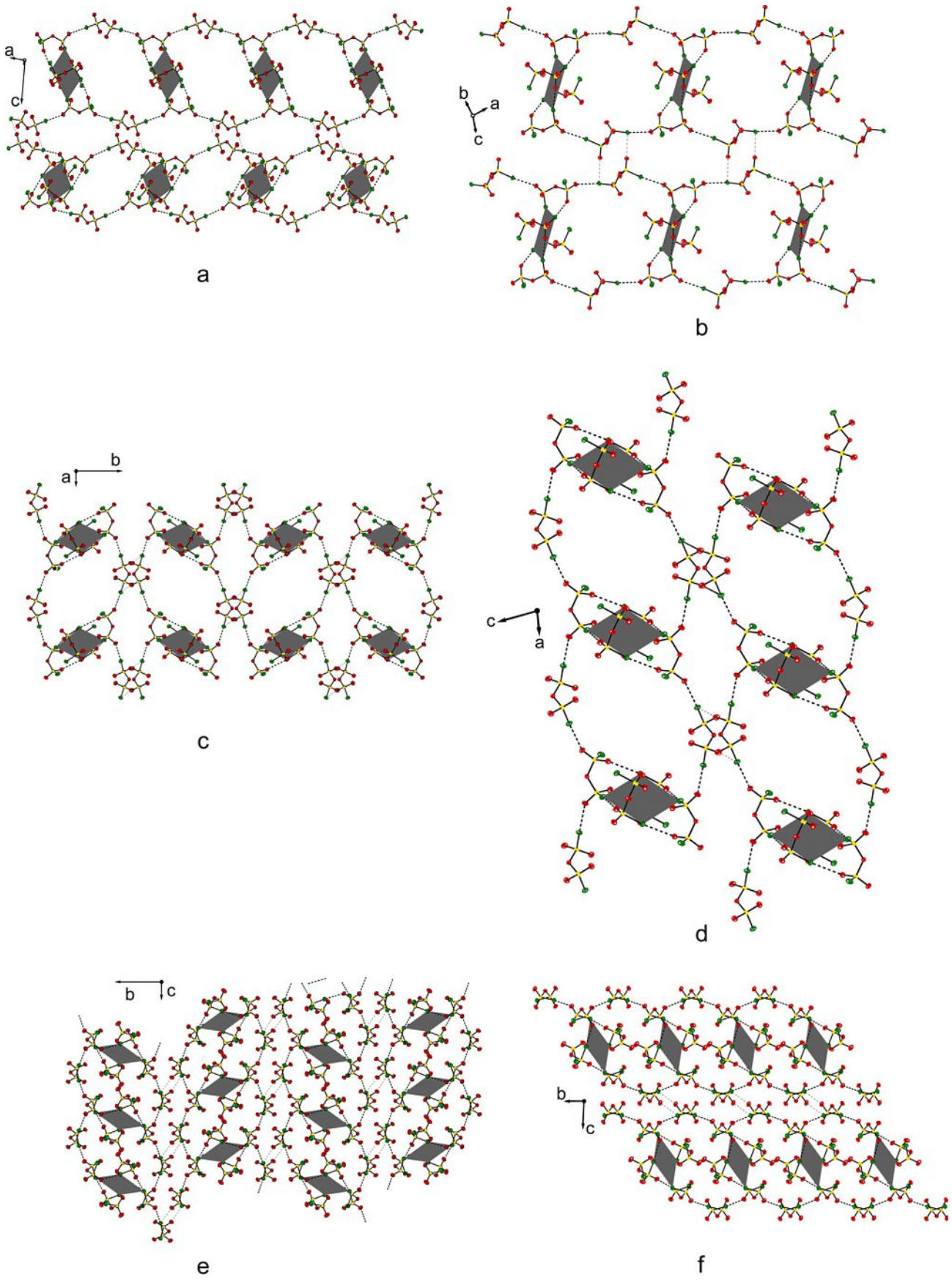

Figure 14. Arrangement of the rope ladders (a,c) in modification 3 and (b, d) modification 4 looking (a, b) roughly at the planes and (c, d) along the 9.44 Å axis and (e, f) along the *a*-axes with ca. 7.6 Å of $ClSO_2OSO_2Cl$. The weaker contacts, that is, 3e und f resp. 4 e and f, are shown as small dotted lines.

in the difluoride (144.9(1)°) than in the dichloride, on average, which is likely due to the higher steric demand of the chlorine atoms.

No directed interactions of the molecules among each other are reported for FSO_2OSO_2F. By contrast, the related disulfuric acid $HOSO_2OSO_2OH$,[20] is composed of three crystallographically independent molecules in the asymmetric unit of its crystals, of which two possess molecular C_2 symmetry. The averaged central S–O bond length at 1.617 Å is between those of the difluoride and the dichloride. Comparing the central S-O-S angles, the acid exhibits the smallest one with 122.1° (averaged). Its extended structure in the solid state is aggregated due to hydrogen bonds. Four molecules form a 24-membered ring of C_2 symmetry. Thus, the dichloride shows similarities with both related compounds, the free acid and the fluoride, with regards to the asymmetric unit.

The above described aggregation by non-covalent interactions in disulfuryl dichloride occur all by O···Cl contacts. These contacts can be characterized as halogen bonding[21] involving chlorine as acceptor and oxygen as donor. Characteristic for halogen bonds is the distance between the interacting atoms, the angle ∡(S–Cl···O) at the acceptor-halogen atom which should be ideally 180° for a σ-hole-type interaction,[22] and the angle at the donor-atom, oxygen ∡(S–O···Cl), which is expected to be bent to represent the position of electron density accumulation at oxygen.

A full listing of the structural parameters of all Cl···O distances below the sum of their van der Waals radii can be found in Table 5. The relation among the individual geometrical parameters is depicted in Figure 15. A distinction between the shortest contacts of each chlorine atom to an oxygen atom and longer ones nevertheless being lower than the sum of the van der Waals radii (3.32 Å) allows a classification into primary and secondary contacts, respectively. The majority of the primary contacts show distances of about 3 Å, ∡(S–Cl···O) angles varying at about 140° and ∡(S–O···Cl) between 160° and 180°. Thus, the highly directional character of the halogen bond is proven in this case as well. The shortest contacts are observed at a Cl···O contact donated by the third molecule in the asymmetric unit of modifications 3 and 4. These links amount to 2.893(1) Å (❸c) and 2.887(1) Å (❹c) with angles of indistinguishable angles at the oxygen atom of 174.9(1)°. The ∡(S–Cl···O) exhibits the same value in both modification within the error ranges, 164.7(1)° and 164.8(1)° for modifications 3 and 4, respectively.

The S–Cl bond lengths belonging to these contacts are the second and third shortest found in this study measuring 1.967(1) and 1.969(1) Å in modifications 3 and 4, respectively. However, primary contacts with Cl···O distances longer than 3.2 Å can be found as well. Three of these four (❸h, ❸j, ❹i; fourth: ❹g) show a systematic correlation between the Cl···O distance and the angles concerning the halogen bond. Along with the increasing of the Cl···O distance, the ∡(SCl···O) angle decreases form 156.3(1)° (❸h) to 97.7(1)° (❸j) whereas the ∡(SO···Cl) angle increases from 133.8(1)° in ❸h to 155.5(1)° in ❸j. This is a tendency observed for halogen bonding: a lower angle at the halogen atom is related to a shorter distance of the contact. Concerning the effect of the halogen bond on the S–Cl bond an increase of the bond length by a longer Cl···O contact can be derived from Figure 15. This is a contradicting fact to the concept of halogen bonding as in such cases an elongation of the covalent bond to a halogen atom is observed when the Lewis base is draw closer to the halogen atom.[22]

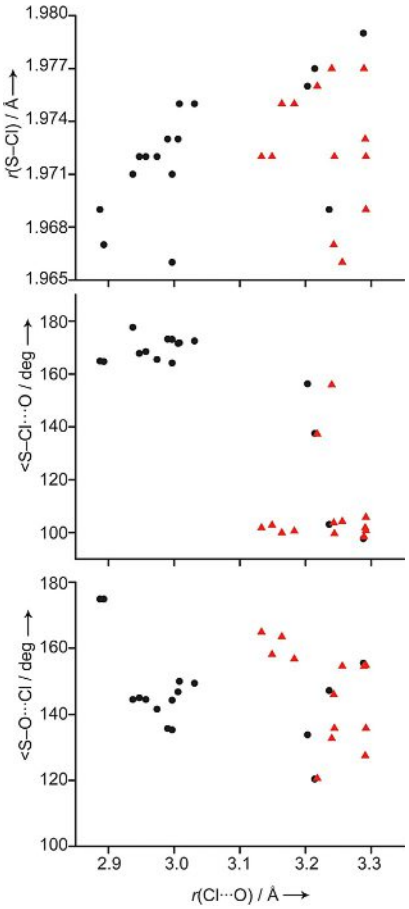

Figure 15. Depiction of the parameters concerning the halogen bonds Cl···O of $ClSO_2OSO_2Cl$. Angles ∡(S–O···Cl) and ∡(S–Cl···O) in °, distances *r*(Cl···O) and *r*(S–Cl) in Å. Black dots stand for the shortest contact of each chlorine atom (primary) whereas the red triangles indicate Cl···O with a longer distance than the shortest one but less than the sum of the van der Waals radii (secondary).

The secondary contacts (red triangles in Figure 15) show all distances above 3.1 Å. The ∡(S–Cl···O) angles are mostly found to be about 100° but in no other chart of Figure 15 common features are recognized as the parameters are spread very strongly.

Electron-density topology

An experimental determination of the charge density distribution $\rho(\boldsymbol{r})$ is possible using high-angle X-ray diffraction data obtained at low temperature.[24] The topological analysis based on Bader's quantum theory of atoms in molecules (QTAIM)[25] allows a quantitative interpretation and description of bonding

and non-bonding interactions. The crystal obtained for modification 1 was of sufficient quality to perform such experiments.

Comparing the computational results with the experimentally determined ones (Table 6) the values of the electron density

Table 6. Intramolecular QTAIM parameters at the bcps for disulfuryl dichloride experimentally determined by high angle X-ray diffraction and by quantum-chemical calculations (exp/qc) for the free molecule.

Bond	$\rho(\boldsymbol{r}_{bcp})$	$-\nabla^2\rho(\boldsymbol{r}_{bcp})$	ε
O1–S1	1.47(2)/1.42	9.57(6)/8.74	0.08/0.07
O1–S2	1.54(2)/1.42	10.75(5)/8.74	0.11/0.07
S1–O2	2.26(2)/2.22	−4.61(11)/−20.39	0.04/0.04
S1–O3	2.42(2)/2.23	11.05(11)/−20.74	0.04/0.05
S1–Cl1	1.12(1)/1.07	0.32(2)/2.55	0.10/0.04
S2–O4	2.34(2)/2.23	−0.79(11)/−20.74	0.13/0.05
S2–O5	2.62(2)/2.22	27.05(1)/−20.39	0.06/0.04
S2–Cl2	1.18(1)/1.07	−0.07(2)/2.55	0.11/0.04

Charge densities $\rho(\boldsymbol{r})$ in $e\,Å^{-3}$, the Laplacians $-\nabla^2\rho(\boldsymbol{r})$ in $e\,Å^{-5}$ and dimension-free bond ellipticities ε. Quantum-chemical calculations were performed at the dispersion-corrected B3LYP-D3/6–311G(2df) level of theory.

$\rho(\boldsymbol{r})$ are very much consistent despite the deviation from molecular C_2 symmetry in the solid-state structure. The most striking differences in the experimentally determined electron density are the values at the bond critical points (bcp) of bonds between sulfur and the terminal oxygen atoms. The experimental values vary between 2.26(2) $e\,Å^{-3}$ and 2.62(2) $e\,Å^{-3}$, whereas the calculated are in all cases approximately the same (2.22 or 2.23 $e\,Å^{-3}$). The S–O bonds exhibiting the lower electron densities at the bcp in both branches of the molecule is located approximately in line with the central S-O-S triangle [ϕ(O2-S1-O1-S2) = 17.0(1)°; ϕ(O4-S2-O1-S1) = 18.1(1)°]. Nevertheless the charge densities at the bond critical points of the S–O bonds involved in the Cl···O contacts is on the one hand the lowest observed here ρ_{bcp}(S1O2) = 2.26(2) $e\,Å^{-3}$ and on the other hand the highest found in the other branch ρ_{bcp}(S2O5) = 2.62(2) $e\,Å^{-3}$. Other experimentally determined electron density distributions of sulfur and oxygen-containing compounds offer a comparison to the molecule examined here. For example, the sulfate ion[26] SO_4^{2-} shows a slightly lower electron density at the critical points of the S–O bond in the range of 2.017 to 2.038 $e\,Å^{-3}$ compared to the respective values of the terminal S–O bond in the dichloride examined here. Otherwise the topological analysis of the electron density of sulfur dioxide[27] exhibits a closer relationship to the molecule examined here regarding the electron density at the ring critical points. In sulfur dioxide this is 2.216(29) $e\,Å^{-3}$ at the bcp and thus very close to the value of the terminal S–O. Therefore, the SO_2 moieties in disulfuryl dichloride seem to be more comparable to the sulfur dioxide than to the sulfate ion judged on the electron density at the critical points of the S–O bonds.

Regarding the Laplacian function of the electron density $-\nabla^2\rho(\boldsymbol{r})$, the computationally determined electron density of a free molecule at the B3LYPD3/6–311G(2df) level of theory fails to reproduce the experimental values. However, the values at the critical points involving the bridging oxygen atom are well reproduced ($-\nabla^2\rho(\boldsymbol{r})_{qc} = 8.74\ e\,Å^{-5}$; $-\nabla^2\rho(\boldsymbol{r})_{exp} = 9.57(6)\ e\,Å^{-5}$ and $-10.75(5)\ e\,Å^{-5}$) and thus the discrepancy in the peripheral bond might originate in the intermolecular interactions as the Laplacian is very sensitive to small changes in the electron density itself. The negative values indicate a covalent character of the bonds. However, the Laplacian at the critical points of the bonds to the terminal oxygen atoms vary heavily between 27.05(1) $e\,Å^{-5}$ and $-4.61(11)\ e\,Å^{-5}$. The increase in the Laplacian is in line with the decreasing value of the electron density at the regarding bcp. Examining the properties of the experimental electron density for the non-covalent interactions of the chlorine and the oxygen atom both interactions feature a very low and similar electron density at the bond critical point of 0.07(1) $e\,Å^{-3}$ and 0.08(1) $e\,Å^{-3}$. Furthermore, the Laplacian at the bcp is in both cases negative $-1.03(1)\ e\,Å^{-5}$ and $-1.05(1)\ e\,Å^{-5}$ that is indicating a non-covalent interaction in this region (Table 7). Regarding the distance of the atomic positions, in comparison to hydrogen bonds as the archetype of non-covalent interactions, the hydrogen atoms show in general higher electron densities in the critical points ($0.10\ e\,Å^{-3} \leq \rho(\boldsymbol{r}) \leq 0.25\ e\,Å^{-3}$) whereas the value of the Laplacian at the bcp is between 2 and 5 $e\,Å^{-5}$. This indicates a higher covalent character in hydrogen bridges than in the here examined chlorine···oxygen contacts.

Table 7. Parameters for the primary intermolecular interactions of two disulfuryl chloride units.

Bond	d(Cl-bcp)	d(O-bcp)	$\rho(\boldsymbol{r}_{bcp})_{exp}$	$-\nabla^2\rho(\boldsymbol{r}_{bcp})_{exp}$	ε_{exp}
Cl1···O5′	1.586	1.389	0.07(1)	1.03(1)	0.10
Cl2···O2″	1.558	1.381	0.08(1)	1.05(1)	0.07
rcp			0.03	0.3	

Charge densities $\rho(r)$ in $e\,Å^{-3}$, the Laplacians $-\nabla^2\rho(r)$ in $e\,Å^{-5}$ and bond ellipticities ε without dimensions.

Conclusions

The conformational conundrum of disulfuryl dichloride was answered by two methods. While in the temperature dependent matrix-isolated vibrational spectra different conformers could be identified, the refinement of the gas-phase diffraction data utilized only one conformer. Furthermore, it is interesting to see the variation of structure parameters between all the eight crystallographically different molecules within the four modifications. This defines the range one has to expect for a certain parameter, if one attempted to answer the simple question "what value does this parameter adopt within this molecule (e.g. the S–Cl bond length)" by a crystallographic measurement. The intermolecular interactions in a crystal may vary parameters among different crystallographically independent molecules. Taking these weak interactions not into account, might give grossly misleading answers. The range in which we determined these parameters are about ten times larger than the least squares standard deviation derived for an individual parameter of one of these molecules. It is the fortunate case of a substance which grows four different modifications of crys-

talline material from an identical sample upon slight variation in the growth conditions, which allows investigating this. For most compounds investigated by single crystal X-ray diffraction we know only one modification and consequently only a little part of the "truth". Based on the topological features derived from the experimental electron density measurement the Cl···O interaction could be classified as a non-covalent one, which is less covalent than hydrogen bridges.

Experimental Section

Synthesis: Disulfuryl dichloride, $ClSO_2OSO_2Cl$, was synthetized by heating an excess of 10 mmol of CCl_4 with 10 mmol of SO_3 for 2 h at 80 °C under permanent stirring. The colorless product was isolated by several trap-to-trap distillations with U-traps kept at −80, −110 and −196 °C (liquid nitrogen). The desired product was concentrated in the trap kept at −80 °C and its purity was conveniently checked using FT-IR spectroscopy.

SO_3 was prepared by heating a reactor containing $M_2S_2O_8$ (M = Na, K) at 270 °C to obtain either $K_2S_2O_7$ or $Na_2S_2O_7$. These salts were subsequently heated with a Bunsen burner to generate SO_3, which was collected in its trimeric form in a U-trap kept at −196 °C. The trimer was subsequently transformed into its monomer through a tube (15 cm length, 1.5 cm diameter) at approximately 120 °C under vacuum conditions.

Different preparations and subsequent comparative spectroscopic evaluation were done to ensure reliability in the identity of the compound. Alternative photochemical preparation methods were the following. a) SO_2, Cl_2 and O_2 were combined and irradiated with light of $\lambda > 320$ nm[3] at −78 °C; b) a mixture of SO_2Cl_2 and SO_3 was irradiated with light of $\lambda > 320$ nm at temperatures of about −50 °C.

Infrared spectroscopy: Infrared (IR) spectra were recorded in Wuppertal on a Bruker Vector 25 spectrometer with a resolution of 1 cm^{-1} in the range from 4000 to 400 cm^{-1}, using a glass cell with Si windows and an optical path length of 10 cm. In La Plata a Thermo Nexus Nicolet FTIR was used. This instrument is equipped with an MCTB detector for the ranges 4000–400 cm^{-1}. A 10 cm gas cell with Si windows was employed.

Matrix isolation: For matrix isolation experiments in Wuppertal, a few milligrams of $ClSO_2OSO_2Cl$ were condensed into a U-trap connected to an inlet nozzle of the matrix equipment, consisting of a quartz tube of internal diameter of 4 mm and an outlet opening of 1 mm diameter,. An Ar flux of 2 mmol h^{-1} was directed to the sample held at −65 °C, and the mixture was deposited on the cold matrix support (15 K, Rh-plated copper block) in a high vacuum. Temperature-dependent experiments were carried out by passing mixtures of the gaseous sample and argon through a quartz nozzle (1 mm i.d.), heated over a length of ~10 mm with a platinum wire (0.25 mm o.d.) prior to deposition on the matrix support. The nozzle was held at 20, 295 or 380 °C.

Photolysis experiment attempts in La Plata were performed using a Spectra-Physics Hg-Xe arc lamp to irradiate the matrix in the broad 200–800 nm range operating at 1000 W. The gas mixture was deposited on a 15 K CsI window using the pulse deposition technique. The low temperature was achieved by means of a Displex closed-cycle refrigerator (SHI-APD Cryogenics, model DE-202). In order to avoid matrix heating, a water filter was placed between the lamp and the matrix. Several spectra were recorded at different irradiation times.[28]

Raman spectroscopy: Raman spectra of the neat liquid (room temperature) was measured in flame-sealed capillaries (3 mm o.d.) on a Bruker RFS 106/S spectrometer, equipped with a 1064 nm Nd:YAG laser, in the region from 4000 to 100 cm^{-1} at a resolution of 4 cm^{-1}.

Gas-phase electron diffraction experiment: The electron diffraction patterns were recorded on the heavily improved Balzers Eldigraph KD-G2 gas-phase electron diffractometer at Bielefeld University. Experimental details are listed in Table 8, instrumental details are reported elsewhere.[29] The electron diffraction patterns, three for each, long and short, nozzle-to-plate distance were measured on the Fuji BAS-IP MP 2025 imaging plates, which were scanned by using calibrated Fuji BAS.1800II scanner. The intensity curves (Figure 16) were obtained by applying the method described earlier.[30] Sector function and electron wavelength were refined[31] using carbon tetrachloride diffraction patterns, recorded in the same experiment as the substance under investigation.

Gas-phase structural analysis: The structural analysis was performed using the UNEX program.[32] All refinements were performed using two averaged intensity curves simultaneously (Figure 16), one for the short and another for the long nozzle-to-plate distance, which were obtained by averaging independently measured intensity curves. For the definition of independent geometrical parameters and their groups in the least-squares refine-

Table 8. Details of the gas-phase electron diffraction experiment for $ClSO_2OSO_2Cl$.

Parameters	Short detector distance	Long detector distance
nozzle-to-plate distance [mm]	250.0	500.0
accelerating voltage [kV]	60	60
fast electron current, [μA]	1.48	1.49
electron wavelength[a] [Å]	0.048632	0.048566
nozzle temperature [K]	293	292
sample pressure[b] [mbar]	2.7×10^{-6}	2.3×10^{-6}
residual gas pressure[c] [mbar]	1.1×10^{-7}	1.2×10^{-7}
exposure time [s]	10	10
used s range [$Å^{-1}$]	6.6 to 32.0	2.4 to 16.0
number of inflection points[d]	4	3
R_f factor	3.389	3.386

[a] Determined from CCl_4 diffraction patterns measured in the same experiment. [b] During the measurement. [c] Between measurements. [d] Number of inflection points on the background lines.

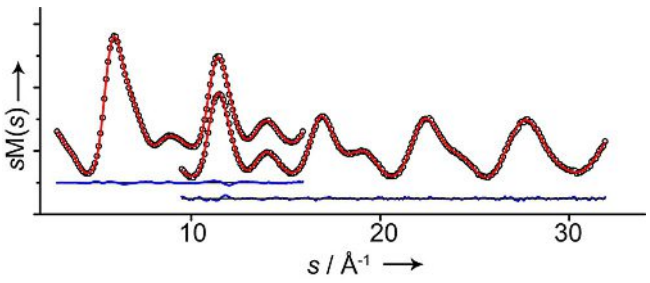

Figure 16. Experimental (dots) and model (solid line) molecular intensity curves of $ClSO_2OSO_2Cl$ for long (upper trace) and short (lower trace) nozzle-to-detector distance and the difference curves, respectively.

ment see Table 6. The *anti*-conformer was assumed to be of C_2 symmetry. The differences between values of parameters were kept fixed at the values taken from the MP2/aug-cc-pVTZ calculations. Start values for amplitudes of vibrations and curvilinear corrections used in the gas-phase electron-diffraction refinements, were calculated using analytical quadratic and numerical cubic force fields for all conformers employing the B3PW91/aug-cc-pVTZ approximation. The mean square amplitudes and vibrational corrections to the equilibrium structure were calculated using the SHRINK program.[33]

X-ray crystallography

A small amount of $ClSO_2OSO_2Cl$ was condensed into a glass capillary (0.3 mm i.d.). This was flame sealed and mounted onto the diffractometer. A single crystal specimen of modification 2 was grown in situ[34] at 234 K, cooled to 232 K at a rate of 1 K h^{-1}, to 225 K at 5 K h^{-1} and to 100 K at 10 K h^{-1}. After heating the capillary to 234 K a single crystal of modification 3 was grown at 234 K, cooled to 232 K at 1 K h^{-1}, to 200 K at 5 K h^{-1} and to 100 K at 10 K h^{-1}. Thawing the sample and growing in situ a crystal at 234 K, cooling to 200 K at 2 K h^{-1} resulted in a crystal of oxonium perchlorate. By examination (optical and due to weak scattering) this was a small crystal solvated by undercooled $ClSO_2OSO_2Cl$. Cooling the sample to 100 K at 10 K h^{-1} polycrystalline $ClSO_2OSO_2Cl$ was identified besides the oxonium perchlorate. After thawing the sample and fast crystallizing without longitudinal translation of the capillary perpendicular to the nitrogen stream at 234 K the cell of modification 2 could be indicated. Again, thawing the crystal and crystallizing at 234 K with longitudinal translation of the crystal, cooling to 233 K at 1 K h^{-1}, to 200 K at 33 K h^{-1} and to 100 K at 33 K h^{-1} resulted in a crystal of modification 4. Thawing the sample to 235 K the cell of modification 3 could be indicated. Warming the capillary to 275 K and growing in situ a single crystal at 233 K and cooling at 33 K h^{-1} to 100 K resulted in formation of a crystal of modification 1. This modification was used to perform an electron density determination. Warming the sample and crystallizing at 234 K, cooling to 200 K at 360 K h^{-1} resulted in the same cells as modification 3 and 4.

All suitable crystals of $ClSO_2OSO_2Cl$ measured on an Agilent SuperNova, Single Source at offset, Eos diffractometer using $Mo_{K\alpha}$ radiation ($\lambda = 0.71073$ Å) at 100.0(1) K. Using Olex2,[35] the structures were solved with the ShelXD[36] structure solution program using Dual Space and refined with the ShelXL[36] refinement package using least-square minimization except modification 1, which was refined using XD-2006.[37] All atoms were refined anisotropically. For the charge density analysis high angle data were obtained up to a resolution of 0.4 Å with high redundancy and completeness (redundancy 36/16, completeness 99.8/98.1% for all data resp. data of the outer range from 0.41 to 0.4 Å). The data were corrected for absorption using SADABS.[38] 8773 reflections with [$I > 3\sigma(I)$] out of 10694 unique reflections were used for refinement. A correction for isotropic extinction[39] was applied, the coefficient refined to 0.0033(6). During the last cycles all multipoles up to hexadecapoles, the κ-values, the extinction coefficient and the positional and anisotropic displacement parameters were refined simultaneously. The local coordinates system and plots produced by WINGX[40] about distribution of outliers, normal probability and fractal dimension can be found in SI. More details are listed in Table 9. CCDC 1582763, 1582764, 1582765, 1582766 and 1582767 contain the supplementary crystallographic data for this paper. These data can be obtained free of charge from The Cambridge Crystallographic Data Centre.

Table 9. Summary of crystallographic data for $ClSO_2OSO_2Cl$.

Modification	1	2	3	4[c]
M_r	215.02	215.02	215.02	215.02
crystal system	monoclinic	monoclinic	monoclinic	Triclinic
space group	$P2_1/c$ (No.14)	$P2_1/c$ (No.14)	$P2_1/c$ (No.14)	$P\bar{1}$ (No.2)
a [Å]	9.91418(3)	5.89383(5)	7.61945(6)	7.6122(5)
b [Å]	10.45034(5)	17.44356(6)	28.2949(2)	9.4474(4)
c [Å]	6.28941(3)	6.29410(3)	9.44053(8)	14.4635(11)
α [°]	90	90	90	83.900(5)
β [°]	101.1373(4)	93.2721(6)	107.8785(9)	78.459(7)
γ [°]	90	90	90	72.117(5)
V [Å^3]	639.353(5)	646.038(7)	1937.02(3)	968.76(11)
Z	4	4	12	6
Z'	1	1	3	3
T [K]	100.0(1)	100.0(1)	100.0(1)	100.0(1)
ρ_{calc} [mg mm^{-3}]	2.234	2.211	2.212	2.211
μ [mm^{-1}]	1.616	1.599	1.600	1.599
$2\Theta_{max}$ [°]	127.2	120.1	120.2	60.1
Index range h	−24–24	−13–14	−18–18	−10–10
Index range k	−26–26	−42–42	−69–69	−13–13
Index range l	−15–15	−15–15	−21–23	−20–20
Refl. collect.	42 1085	43 7080	511667	6978
Indep. refl.	10694	9830	29430	6978
R_{int}	0.0312	0.0472	0.0442	0.0456
Data/restraints/parameters	8773/0/311	9830/0/83	29430/0/245	6978/0/246
R_1, $I > 2\sigma(I)$/all data	0.0147/0.021	0.0236/0.0283	0.0351/0.0483	0.0324/0.0350
wR_2, $I > 2\sigma(I)$/all data	0.0235/0.0239	0.0640/0.0665	0.0763/0.0801	0.1087/0.1112
GoF	2.392	1.077	1.116	1.075
$\rho_{max/min}$ [e Å^{-3}]	0.37/−0.30	1.21/−0.97	0.79/−0.84	0.67/−0.63
CCDC	1582764	1582763	1582766	1582765

[a] R_1 is defined as $\Sigma||F_o|-|F_c||/\Sigma|F_o|$ for $I > 2\sigma(I)$. [b] wR_2 is defined as $[\Sigma w\{F_o^2-F_c^2\}^2/\Sigma w(F_o^2)^2]^{1/2}$ for $I > 2\sigma(I)$. [c] Crystal was a non-merohedral twin, ratio 85:15. Both domains were taken into account for data integration and refinement.

Quantum-chemical calculations. A potential energy scan was performed at the O3LYP[9,16] level of density functional theory with the correlation-consistent cc-pVTZ[10] basis set on the Firefly[41] program suite. Full optimisations were performed using the Gaussian 09.D01 version[42] and the respective MP2[11] method with the given basis set. The theoretical electron density distribution was performed on the B3LYP[13]-D3[43] level with the 6-311G(2df) basis set using the AIMALL program.[44]

Acknowledgements

This work was supported by Deutsche Forschungsgemeinschaft (DFG, core facility GED@BI, grant MI477/35-1). RMR and CODV thank Agencia Nacional Científica *y* Tecnológica ANPCyT (PICT14-3266 and PICT14-2957), Facultad de Ciencias Exactas of the Universidad Nacional de La Plata (UNLP-11/X684 and UNLP-11/X713) and Consejo Nacional de Investigaciones Científicas *y* Técnicas CONICET (PIP-0352 and PIP-0348) for financial support. R.M.R. also thanks for a DAAD fellowship.

Conflict of interest

The authors declare no conflict of interest.

Keywords: disulfuryl dichloride · gas-phase electron diffraction · in situ crystallization · matrix-isolation vibrational spectroscopy · solid-state modifications

[1] R. J. Gillespie, E. A. Robinson, *Can. J. Chem.* **1961**, *39*, 2179.
[2] M. A. Grela, A. J. Colussi, *J. Phys. Chem.* **1996**, *100*, 10150.
[3] R. M. Romano, C. O. Della Védova, H. Beckers, H. Willner, *Inorg. Chem.* **2009**, *48*, 1906.
[4] A. M. Betancourt, Y. B. Bava, Y. B. Martinez, M. F. Erben, R. L. C. Filho, C. O. Della Vedova, R. M. Romano, *J. Phys. Chem. A* **2015**, *119*, 8021.
[5] W. Prandtl, P. Borinski, *Z. Anorg. Chem.* **1909**, *62*, 24.
[6] R. J. Gillespie, E. A. Robinson, *Spectrochim. Acta* **1963**, *19*, 741.
[7] J. L. Hencher, S. H. Bauer, *Can. J. Chem.* **1973**, *51*, 2047.
[8] A. J. Blake, Z. Žák, *Acta Crystallogr. Sect. C* **1993**, *49*, 7.
[9] A. J. Cohen, N. C. Handy, *Mol. Phys.* **2001**, *99*, 607.
[10] R. A. Kendall, T. H. Dunning, R. J. Harrison, *J. Chem. Phys.* **1992**, *96*, 6796.
[11] C. Møller, M. S. Plesset, *Phys. Rev.* **1934**, *46*, 618.
[12] R. J. Gillespie, E. A. Robinson, *Can. J. Chem.* **1964**, *42*, 2496.
[13] A. D. Becke, *Phys. Rev. A* **1988**, *38*, 3098.
[14] a) J. P. Perdew, *Phys. Rev. B* **1986**, *33*, 8822; b) J.-P. Blaudeau, M. P. McGrath, L. A. Curtiss, L. Radom, *J. Chem. Phys.* **1997**, *107*, 5016; c) M. M. Francl, W. J. Pietro, W. J. Hehre, J. S. Binkley, M. S. Gordon, D. J. DeFrees, J. A. Pople, *J. Chem. Phys.* **1982**, *77*, 3654; d) V. A. Rassolov, M. A. Ratner, J. A. Pople, P. C. Redfern, L. A. Curtiss, *J. Comput. Chem.* **2001**, *22*, 976.
[15] A. Simon, R. Lehmann, *Z. Anorg. Allg. Chem.* **1961**, *311*, 212.
[16] C. Lee, W. Yang, R. G. Parr, *Phys. Rev. B* **1988**, *37*, 785.
[17] H. Chaabouni, L. Schriver-Mazzuoli, A. Schriver, *J. Phys. Chem. A* **2000**, *104*, 3498.
[18] R. Haist, H. G. Mack, C. O. Védova, E. H. Cutín, H. Oberhammer, *J. Mol. Struct.* **1998**, *445*, 197.
[19] M. Hargittai, I. Hargittai, *J. Mol. Struct.* **1981**, *73*, 253.
[20] W. Hönle, *Z. Kristallogr.* **1991**, *196*, 279.
[21] G. R. Desiraju, P. S. Ho, L. Kloo, A. C. Legon, R. Marquardt, P. Metrangolo, P. Politzer, G. Resnati, K. Rissanen, *Pure Appl. Chem.* **2013**, *85*, 1711.
[22] T. Clark, M. Hennemann, J. S. Murray, P. Politzer, *J. Mol. Model.* **2007**, *13*, 291.
[23] G. Cavallo, P. Metrangolo, R. Milani, T. Pilati, A. Priimagi, G. Resnati, G. Terraneo, *Chem. Rev.* **2016**, *116*, 2478.
[24] a) P. Coppens, *X-ray charge densities and chemical bonding*, International Union of Crystallography, Chester, England, **1997**; b) T. S. Koritsanszky, P. Coppens, *Chem. Rev.* **2001**, *101*, 1583.
[25] a) R. F. W. Bader, *Atoms in Molecules. A Quantum Theory*, Clarendon, Oxford, **2003**; b) R. F. W. Bader, *Chem. Rev.* **1991**, *91*, 893.
[26] M. S. Schmøkel, S. Cenedese, J, Overgaard, M. R. V. Jørgensen, Y.-S. Chen, C. Gatti, D. Stalke, B. B. Iversen, *Inorg. Chem.* **2012**, *51*, 8607.
[27] S. Grabowsky, P. Luger, J. Buschmann, T. Schneider, T. Schirmeister, A. N. Sobolev, D. Jayatilaka, *Angew. Chem. Int. Ed.* **2012**, *51*, 6776; *Angew. Chem.* **2012**, *124*, 6880.
[28] a) I. R. Dunkin, *Matrix-isolation techniques. A practical approach*, Oxford Univ. Press, Oxford, **1998**; b) M. J. Almond, A. J. Downs, *Spectroscopy of Matrix Isolated Species, Vol. 17 of Advances in Spectroscopy*, Wiley, Chichester, **1989**; M. J. Almond, A. J. Downs, *Spectroscopy of Matrix Isolated Species, Vol. 17 of Advances in Spectroscopy*, Wiley, Chichester, **1990**; c) R. N. Perutz, J. J. Turner, *J. Chem. Soc. Faraday Trans. 2* **1973**, *69*, 452.
[29] a) C. G. Reuter, Y. V. Vishnevskiy, S. Blomeyer, N. W. Mitzel, *Z. Naturforsch. B* **2016**, *71*, 1; b) R. J. F. Berger, M. Hoffmann, S. A. Hayes, N. W. Mitzel, *Z. Naturforsch. B* **2009**, *64*, 1259.
[30] Yu. V. Vishnevskiy, *J. Mol. Struct.* **2007**, *833*, 30.
[31] Yu. V. Vishnevskiy, *J. Mol. Struct.* **2007**, *871*, 24.
[32] Y. V. Vishnevskiy, "UNEX, v. 1.6.0", http://unexprog.org, **2013**.
[33] a) V. A. Sipachev, *J. Mol. Struct. THEOCHEM* **1985**, *121*, 143; b) V. A. Sipachev, *J. Mol. Struct.* **2001**, *567–568*, 67; c) V. A. Sipachev, *J. Mol. Struct.* **2004**, *693*, 235.
[34] R. Boese, *Z. Kristallogr.* **2014**, *229*, 595.
[35] O. V. Dolomanov, L. J. Bourhis, R. J. Gildea, J. A. K. Howard, H. Puschmann, *J. Appl. Crystallogr.* **2009**, *42*, 339.
[36] a) G. M. Sheldrick, *Acta Crystallogr. Sect. A* **2015**, *71*, 3; b) G. M. Sheldrick, *Acta Crystallogr. Sect. C* **2015**, *71*, 3.
[37] A. Volkov, P. Macchi, L. J. Farrugia, C. Gatti, P. R. Mallinson, Richter, T. Koritsánszky, **2006**, XD2006.
[38] Sadabs **2012/1**, Bruker AXS Inc., Madison, Wisconsin, USA.
[39] P. J. Becker, P. Coppens, *Acta Crystallogr. Sect. A* **1974**, *30*, 129.
[40] L. J. Farrugia, *J. Appl. Crystallogr.* **2012**, *45*, 849.
[41] A. A. Granovsky, "Firefly version 7.1.G", http://classic.chem.msu.su/gran/firefly/index.html.
[42] Gaussian 09 (Revision D.01), M. J. Frisch, G. W. Trucks, H. B. Schlegel, G. E. Scuseria, M. A. Robb, J. R. Cheeseman, G. Scalmani, V. Barone, B. Mennucci, G. A. Petersson, H. Nakatsuji, M. Caricato, X. Li, H. P. Hratchian, A. F. Izmaylov, J. Bloino, G. Zheng, J. L. Sonnenberg, M. Hada, M. Ehara, K. Toyota, R. Fukuda, J. Hasegawa, M. Ishida, T. Nakajima, Y. Honda, O. Kitao, H. Nakai, T. Vreven, J. A. Montgomery, Jr., J. E. Peralta, F. Ogliaro, M. Bearpark, J. J. Heyd, E. Brothers, K. N. Kudin, V. N. Staroverov, R. Kobayashi, J. Normand, K. Raghavachari, A. Rendell, J. C. Burant, S. S. Iyengar, J. Tomasi, M. Cossi, N. Rega, J. M. Millam, M. Klene, J. E. Knox, J. B. Cross, V. Bakken, C. Adamo, J. Jaramillo, R. Gomperts, R. E. Stratmann, O. Yazyev, A. J. Austin, R. Cammi, C. Pomelli, J. W. Ochterski, R. L. Martin, K. Morokuma, V. G. Zakrzewski, G. A. Voth, P. Salvador, J. J. Dannenberg, S. Dapprich, A. D. Daniels, Ö. Farkas, J. B. Foresman, J. V. Ortiz, J. Cioslowski, and D. J. Fox, Gaussian, Inc., Wallingford CT, **2009**.
[43] L. Goerigk, S. Grimme, *J. Chem. Theory Comput.* **2011**, *7*, 291.
[44] T. A. Keith, "AIMALL (version 16.05.18), TK Gristmill Software Overland Parks KS, USA, http://aim.tkgristmill.com, **2016**.

Manuscript received: February 16, 2018
Accepted manuscript online: April 30, 2018
Version of record online: June 27, 2018